MACROKINETICS OF THE PROCESS OF SHS COMPACTION

V. A. Shcherbakov, A. N. Gryadunov, and A. S. Shteinberg

UDC 621.762

Dependences are considered for the characteristic times of the main stages of the SHS compaction process – synthesis, compaction, and cooling – on the geometric size of a charge billet and the composition of a synthesized hard alloy. The existence is shown of two critical sizes for a starting billet which limit the region of producing a nonporous material. The presence of the critical conditions depending on the liquid phase fraction formed in the synthesis of a hard alloy is established. A satisfactory qualitative and quantitative agreement of calculated and experimental results is obtained.

Introduction. A single-stage production of hard alloys by the method of SHS compaction is a complex macrokinetic problem involving joint consideration of such processes as combustion, heat and mass transfer, compaction, phase formation, and others.

In a general form the process of SHS compaction is realized in the following way [1]. A charge billet pressed from a reaction mixture of powders is placed into a mold. The billet surface is separated from the mold inner surface by the layer of a porous heat insulator. A reaction of synthesis of the target product is locally initiated by a short heat pulse. The reagent interaction occurs in a thin layer separating the starting mixture and the final product. Once initiated, the reaction zone (SHS front) propagates spontaneously over the specimen in the combustion regime. As this takes place, synthesis of the hard-alloy components (high-melting compounds and a binding composition) and heating of the porous specimen necessary for high-temperature treatment by pressing simultaneously occur. Upon completion of the reaction in the entire volume of the billet a heated-up porous hard-alloy material is pressed.

An important feature of SHS compaction is variation in time and, on occasion, in space of the temperature of the compacted material.

At present a considerable amount of experimental data on the production of tungsten-free hard alloys by the method of SHS compaction has been accumulated [2]. Some special features of the process associated with selecting the composition of the reaction mixture [3], phase formation [4], and the influence of degassing processes [5, 6] have been studied, and the regimes of heating for press-attachments have been considered [7]. However, there is still no unified approach explaining the body of experimental results and making it possible to correctly select optimal regimes of compaction. From this point of view the analysis of a thermal regime for the process of producing hard alloys by the SHS compaction method seems topical.

1. Characteristic Times of the Process of SHS Compaction. For analyzing the macrokinetics of SHS compaction it makes sense to introduce into the consideration characteristic times of the main stages of the process: synthesis, compaction, and cooling. We will consider the dependences of these times on the factors determining the production of quality materials.* As will be shown below, the most important of them are the geometric size of the charge billet and the composition of the synthesized product. The billet size appears in the corresponding formulas in an explicit form. The second factor affects the characteristic times of the main stages via the burning rate of the reaction mixture, the dynamic viscosity factor of the synthesized hard alloy as well as its thermophysical characteristics.

Time of Synthesis of Hard Alloy Material. The stage of preparation of a porous specimen for high-temperature treatment by pressing is determined by the time of synthesis of a hard alloy. In this work we will consider charge billets of a cylindrical shape with a constant diameter (D) and height (d) varied within the limits $0 < d/D < 1$.

*In this case "quality" means high density material, in the limit – a nonporous one.

Institute of Structural Macrokinetics, Russian Academy of Sciences, Chernogolovka. Translated from Inzhenerno-Fizicheskii Zhurnal, Vol. 63, No. 5, pp. 583-592, November, 1992. Original article submitted February 9, 1992.

1062-0125/92/6305-1111$12.50

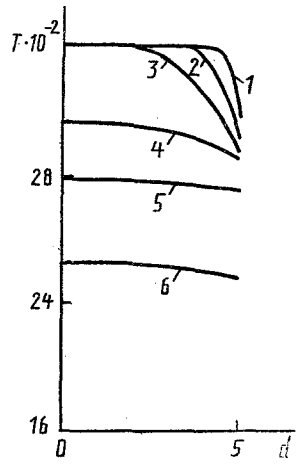

Fig. 1. Temperature distribution across the specimen thickness at various instants on the completion of SHS of the hard-alloy material: 1) 0.001; 2) 0.01; 3) 0.1; 4) 1.0; 5) 7.0; 6) 10 sec. T, K; d, mm. Temperature profiles 1-6 merge into one at d = 5 mm.

Initiating the reaction of synthesis of the hard-alloy material is performed on the lateral (cylindrical) side of the billet. Due to the local initiation of the SHS reaction any other position of a firing coil does not practically lead to a substantial (more than twice as much) decrease of the heating time. The synthesis time of the hard-alloy material was calculated by the formula

$$t_s = D/U. \tag{1}$$

In the calculations we used experimental data on gasless burning rates [8, 9].

Time of Compaction of Hard Alloy. For a description of the deformation of a porous specimen in pressing we will employ model representations developed in [10, 11]. In this connection we will consider that shrinkage of a homogeneous porous material is controlled by the process of viscous flow. With allowance made for the pressure distribution across the thickness of the porous specimen, the compaction time from the initial density $\rho_{in} = 0.5$ to the final one $\rho_f = 0.995$ may be presented in the form

$$t_f = \frac{4}{3}\frac{\eta}{\overline{P}}\int_{\rho_{in}}^{\rho_f}\frac{\rho^3 d\rho}{1-\rho}, \tag{2}$$

where

$$\overline{P} = \frac{P_0 D}{8\xi f d}\left[1 - \exp\left(-8\xi f d/D\right)\right]. \tag{3}$$

The ductility of hard-alloy materials considerably builds up with a liquid phase in their composition. According to [12], it acts as a lubricant making the mutual travel of solid particles easier. In synthesis of a hard-alloy material the liquid phase may form in two cases: in melting of high-melting compounds or eutectics based on them; in melting of a metal binder. The liquid phase fraction can be determined from the equation of heat balance, according to which the heat released during SHS is consumed by heating and melting of the hard alloy components:

$$Q = c_1(T_c - T_0) + \frac{m}{1-m}\left[L + c_2(T_c - T_0)\right]. \tag{4}$$

It was assumed in the calculations that high-melting compounds do not dissolve in a metal binder nor do they form eutectics with it.

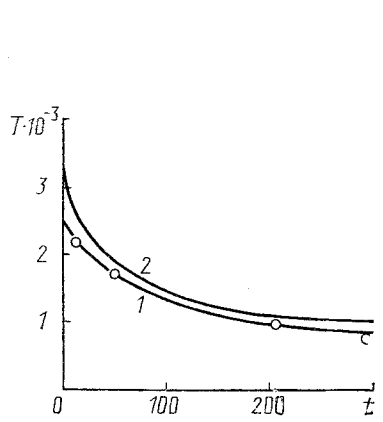

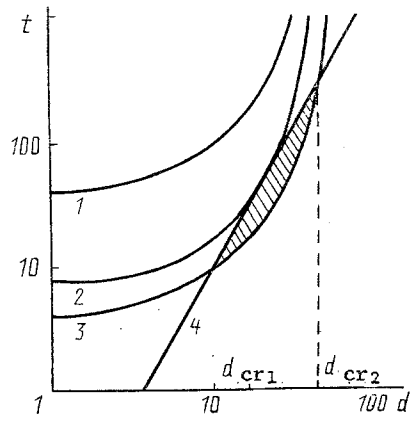

Fig. 2 Fig. 3

Fig. 2. Dynamics of cooling for the layer of synthesized hard-alloyed material containing TiB_2–20% and TiC–80%, placed into quartz sand; the layer thickness is 15 mm. t, sec.

Fig. 3. Calculated dependence of the characteristic times of compaction (1-3) and cooling (4) on the thickness of the charge billet at different dynamic viscosity factors of the synthesized hard alloy TiC–TiB_2: 1) 10^{10}; 2) 10^9; 3) 10^8 P; the parametric region, within which the nonporous hard alloy can be produced, is hatched.

The level of dynamic viscosity of a hard-alloy material is conditioned by the liquid phase contained in it. In the course of SHS the fraction of the latter may vary in a wide range. Procedures described in the literature enable us to calculate the viscosity of suspensions with a solid content up to 40 vol.% [13, 14]. Therefore in this work we used experimental dependences of the characteristic pressing times for hard alloys [5, 15] and of values of dynamic viscosities obtained from these data.

Time of Cooling of Hard Alloy. By the characteristic time of cooling we will mean the time of existence of a liquid phase in the hard alloy. It was calculated from the solution to the known problem of cooling and crystallization of a material layer, placed into a porous medium, for the fourth-kind boundary conditions – the equality of the corresponding temperatures and heat fluxes to the left and to the right from the surface of contact. According to [16], the temperature distribution in the cooling specimen is determined by the expression

$$\theta = 1 - \frac{1}{1+k}\sum_{n=1}^{\infty}(-k)^{k-1}\left\{\operatorname{erfc}\frac{(2n-1)\frac{d}{2}-x}{2\sqrt{a\tau}} + \operatorname{erfc}\frac{(2n-1)\frac{d}{2}+x}{2\sqrt{a\tau}}\right\}. \quad (5)$$

The crystallization time of the liquid phase was taken into account by Eger's method [17] by adding the quantity mL/c to the specimen temperature.

The thermal conductivities were calculated by traditional methods [18, 19] using data [20-22] extrapolated to the high-temperature region. In the process of compacting, the indicated parameters vary since they depend on the density of the hard-alloy material.

A substantial difference in the thermal activities and thermal conductivities of the compacted hard-alloy specimen and of the heat insulator around it causes the corresponding temperature field in the specimen. The results of calculating the temperature distribution across the thickness of the hard-alloy material layer, containing TiB_2–20% and TiC–80%*, are presented in Fig. 1. It can be seen that the specimen cools in the nongradient regime. In this connection, when performing thermal calculations, the average thermophysical characteristics of hard alloys are used, and the temperature in the specimen at each instant is considered constant, independent of the coordinate.

*Hereinafter the composition of the hard alloy is given in wt.%, unless otherwise specified.

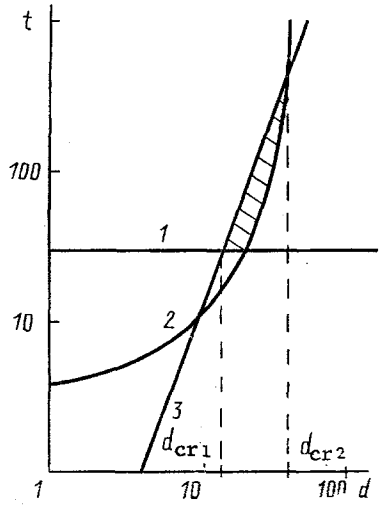

Fig. 4

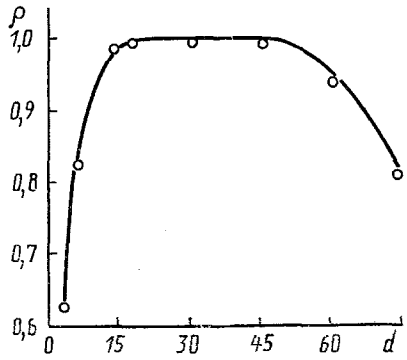

Fig. 5

Fig. 4. Calculated dependences of the characteristic times of synthesis (1), compaction (2), and cooling (3) of the hard alloy containing TiC–80%, TiB_2–20% on the thickness of the charge billet.

Fig. 5. Experimental dependence of the relative density of the hard alloy on the thickness of the charge billet.

Reliability of the performed calculations is confirmed by their agreement with experiment. Figure 2 shows two temperature curves of cooling for the specimen of the hard alloy TiC–TiB_2 (without the stage of pressing). Curve 1 is obtained experimentally in [5]; curve 2 is calculated from Eq. (5). We notice that they are in satisfactory agreement with each other. A small discrepancy between the curves at the initial instant of cooling is related to taking account by Eger's method [17] of a partial melting of the synthesis products.

2. Influence of the Size of a Charge Billet. We will consider the limiting case when the synthesis time of the hard-alloy material is much less than the compaction and cooling times. Figure 3 shows the dependence of the characteristic cooling and pressing times on the thickness of the charge billet at different values of dynamic viscosity of the synthesized hard alloy TiC–TiB_2. It is evident that when the viscosity of the material is large ($\eta_1 = 10^{10}$ P) the intersection of the curves is absent. This indicates that for any geometric size of the billet the cooling time is less than the compaction time.

A decrease in the viscosity of the synthesized material ($\eta_2 = 10^9$ P) leads to the pressing and cooling curves contacting at one point. In this case only one geometric size of the billet exists, with which it is possible to produce a nonporous alloy. Further decrease in the viscosity of the synthesis products ($\eta_3 = 10^8$ P) gives rise to a whole region of such geometric sizes (it is hatched in Fig. 3).

A compact hard-alloy material can be produced when one satisfies the following evident condition:

$$t_s \ll t_c \leqslant t_0. \tag{6}$$

The size of the charge billet for which the condition

$$t_c = t_0 \tag{7}$$

is satisfied will be referred to as critical (d_{cr}).

In compaction by a pressure of 10^8 Pa of a hard-alloy material with $\eta = 10^8$ P the calculated values of d_{cr} are 10 and 50 mm, respectively.

An increase in the time of synthesis of the hard alloy leads to a decrease of the region of geometric sizes for the charge billet within which the production of the nonporous hard alloy is possible (see Fig. 4). It is necessary to point out that in this case the first critical size of the billet is determined by the relation of the characteristic times of synthesis and cooling of the specimen, the second one – by that of compaction and cooling. Further decrease in the burning rate results in violating the condition (6).

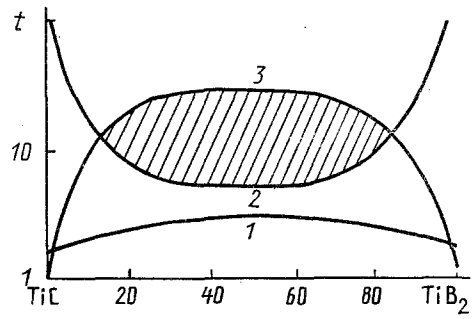

Fig. 6

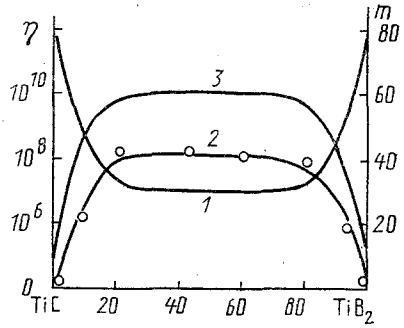

Fig. 7

Fig. 6. Calculated dependences of the characteristic times of synthesis (1), compaction (2), and cooling (3) on the composition of the hard alloy TiC–TiB_2.

Fig. 7. Dependences of the dynamic viscosity factor (1) and the liquid phase fraction (2, experiment; 3, calculation) on the composition of the hard alloy TiC–TiB_2. η, P; m, %.

We will compare the calculated d_{cr} values with the experimental results obtained in [5]. Figure 5 shows the dependence of the relative density of the hard alloy with TiC–80% and $TiB2_2$–20% ($\eta = 3.5 \cdot 10^8$ P) on the thickness of the starting billet. It can be seen that the production of the compact hard alloy with a residual porosity <1% is attained with a billet $15 \leq d \leq 45$ mm thick. By decreasing the thickness of the billet to less than 15 mm or increasing it to more than 45 mm the porosity of the hard alloy material grows. The calculated data obtained are in good qualitative and quantitative agreement with the experiment.

3. SHS Compaction of Hard Alloy of High-Melting Compounds. We will consider SHS compaction of the hard alloy which is comprised only of high-melting compounds using the system TiC–TiB_2 as an example. Figure 6 presents the dependences of the characteristic times of synthesis, compaction, and cooling on the composition of the target product, formed in combustion of the system Ti–C–B. It is obvious that for any relation of the reaction mixture components the time of synthesis of the hard-alloy material is much less than that of compaction and cooling. The condition (6), however, is met in synthesis of the hard alloy with a TiB_2 content of 20 to 80%. This is due to its largest ductility at the synthesis temperature (see Fig. 7, curve 1).

The obtained result can be explained using data on the formation of a liquid phase in the course of SHS of the hard alloy TiC–TiB_2. The dependence of the liquid phase fraction on the composition of the target product is shown in Fig. 7. Curve 2 is obtained from Eq. (4), curve 3 – from experimental data [5]. It can be seen that in combustion of the binary systems Ti–C or Ti–B with only one high-melting compound TiC or TiB_2 formed, melting of the final products does not occur. The dynamic viscosity factor in this case is, on the average, 10^{11} P, which agrees with the viscosity of titanium carbide given in [10] in order of magnitude. Low ductibility of the synthesized material does not permit its compaction to a nonporous state.

In combustion of a three-component reaction mixture a final product forms as a composition of TiC and TiB_2 grains and the liquid phase with euthectic composition. The maximum liquid phase amount of 40 vol. % is attained with a TiB_2 content of 20-80% in the hard alloy. Therefore, the hard alloys mentioned have a minimum viscosity of 10^6-10^7 P.

By analogy, the liquid phase fraction, for which the condition (7) is satisfied, will be referred to as critical. In SHS compaction of the hard alloy TiC–TiB_2 there exist two critical conditions which are observed with 20 and 80% TiB_2 in the hard alloy.

We will compare the results of calculations with experimental values of densities of the hard alloys. Figure 8 shows the dependence of the relative density on the composition of the hard alloy TiC–TiB. It is evident that the porosity of the material formed solely of TiC or TiB_2 is 15-20%. The compact hard alloy with residual porosity less than 1.0% is produced in the synthesis of a two-phase final product with a TiB_2 content within 20-60%. As has been shown above, in this case the necessary amount of the liquid phase is generated (see Fig. 6), which enables us to perform compaction of the synthesized hard alloy during its lifetime.

4. SHS Compaction of a Hard Alloy of a High-Melting Compound and a Metal Binder. We will consider SHS compaction of a hard alloy containing a metal binder using the system TiB–Ti as an example. Figure 9 shows the dependences of the characteristic times of synthesis, compaction, and cooling on the metal binder content. It can be seen that, as in the above-considered hard alloy TiC–TiB_2, independently of the metal binder concentration, the time of synthesis of the hard alloy is much

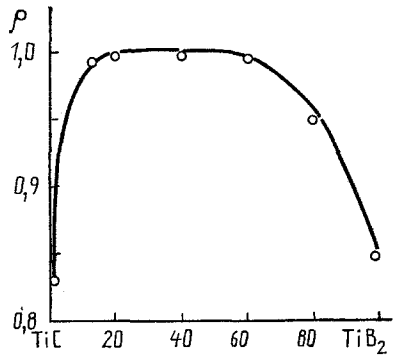

Fig. 8. Experimental dependence of the relative density on the composition of the hard alloy TiC–TiB_2.

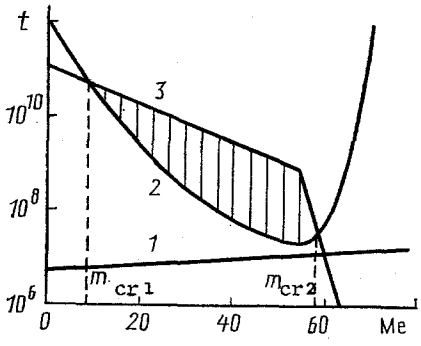

Fig. 9

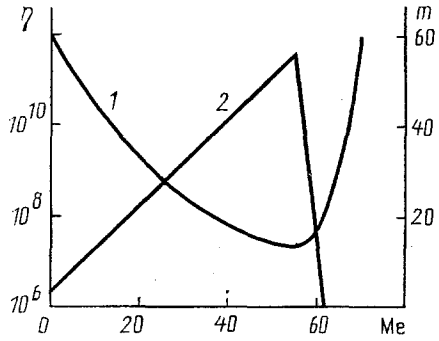

Fig. 10

Fig. 9. Calculated dependences of the characteristic times of synthesis (1), compaction (2), and cooling (3) of the hard alloy TiB–Ti on the metal binder content. Me, wt. %.

Fig. 10. Calculated dependences of the dynamic viscosity factor (1) and the liquid phase fraction (2) on the metal binder content in the hard alloy TiB–Ti.

less than the time of compaction and cooling. The condition (6) is met solely with a certain relation of components, which is linked with the generation of the necessary amount of the liquid phase (see Fig. 9).

If a titanium–boron proportion exists in the starting mixture such that there is no liquid phase in the SHS product then the final product has a large dynamic viscosity (10^{10} P). Compaction of the porous specimen under these conditions is hampered, and the production of a nonporous hard alloy fails (Fig. 10).

Formation of 5-10 vol.% of a melt in the SHS product of TiB–Ti* results in a significant decrease in viscosity. As the metal binder content increases up to 50-60%, the material viscosity decreases down to 10^6-10^7 P. As a result, the rate of deformation for the porous specimen increases and, with the condition (6) met, it is possible to produce a practically nonporous material.

The analogy of SHS compaction of the hard alloy TiB–Ti and TiC–TiB_2 consists in the fact that there also exist two critical conditions depending on the hard alloy composition which in this case differ by the metal binder content. For the hard alloy TiB–Ti the first critical value of the fraction of the titanium binder is 5-10%, the second one – 50% (see Fig. 9).

An unusual situation arises: the synthesized material contains the maximum amount of the melted binder but we fail to produce a hard alloy. This is because increasing the metal binder content in the starting charge leads, on the one hand, to a growth of the liquid phase fraction in the final product, and, on the other, to a decrease of its lifetime due to lowering the combustion temperature. By increasing the binder concentration above critical the condition (6) is violated.

*It was assumed in the calculations that high-melting compounds do not dissolve in a metal binder nor do they form eutectics with it.

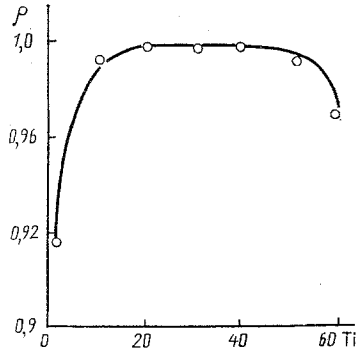

Fig. 11

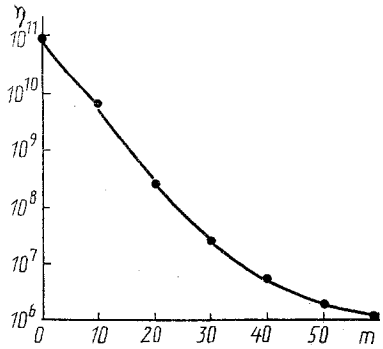

Fig. 12

Fig. 11. Experimental dependence of the relative density of the hard alloy TiB–Ti on the metal binder content. Ti, wt.%.

Fig. 12. Generalized dependence of the viscosity of a highly filled suspension on the liquid phase content. m, vol.%.

We will compare the results obtained with the experimental data of [15]. We notice that the critical values of the liquid phase fraction in SHS compaction of the hard alloy TiB–Ti are equal to 10 and 45 vol.%, respectively. The results obtained are in qualitative and quantitative agreement with experiment (see Fig. 11).

Discussion of the Results. It is of interest to compare the specific features of SHS compaction of ceramic and powdered-metal hard alloys. It is evident that a common feature in both cases is the decisive role of the presence of the liquid phase in the compacted material.

Figure 12 gives a generalized dependence of the viscosity of a highly filled suspension on the liquid-phase content. It can be seen that in a sufficiently wide range of parameter variation an increase in the liquid phase content by 10 vol.% corresponds to a decrease in the suspension viscosity by approximately an order of magnitude.

We will consider the characteristic compaction and cooling times in the production of ceramic and powdered-metal hard alloys. In the first case the liquid phase is generated by melting of an eutectic comprised of high-melting compounds. A special feature of SHS compaction of a ceramic hard alloy is the absence of thermally inertial alloy components, and the heating temperature of a billet during SHS is limited by the melting temperature of the eutectic. It is reasonable that the cooling time of the ceramic hard alloy increases as the liquid phase fraction grows. As a consequence, the curves $\eta = \eta(m)$ corresponding to pressing and cooling intersect only at one point (see Fig. 13). Thus, with a variation of the ceramic hard alloy composition in SHS compaction only one critical value of the liquid phase fraction is observed.

A fundamentally new situation is realized in producing a powdered-metal hard alloy. The liquid phase in the SHS of a hard alloy of this type is generated by melting of the metal binder, which is an inertial diluent. The combustion temperature in this case exceeds, as a rule, the melting temperature for the metal binder. In this connection, for most of the practically interesting systems the cooling time decreases with an increase in the melted binder content. Therefore the pressing and cooling curves intersect at two points (see Fig. 14). Thus, the basic difference of the regimes of SHS compaction of the ceramic and powdered-metal hard alloys is that in the first case only one critical value of the liquid phase fraction is observed and in the second – two.

CONCLUSIONS

1. The thermal regime of SHS compaction is analyzed, in which the characteristic times of the three main stages – synthesis, compaction, and cooling – are recognized. The optimal conditions for producing compact hard alloys are established.

2. The influence of the geometric size of a charge billet on the SHS compaction regimes is considered. The existence of the two critical sizes of the specimen which limit the region of producing nonporous hard alloys is established.

*The dependence $\eta = \eta(m)$ is obtained using the experimental [5, 10, 15] values under the assumption that the solid-phase particles have a spherical shape and are wetted by a liquid phase.

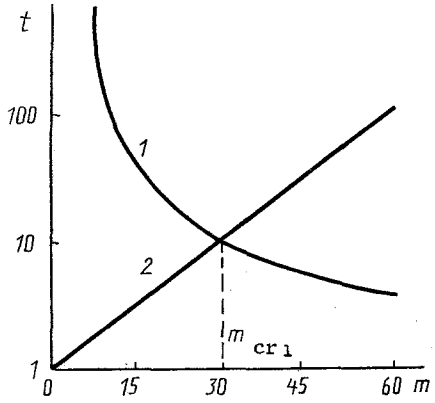

Fig. 13

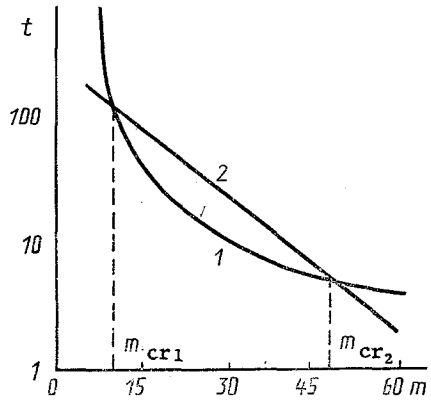

Fig. 14

Fig. 13. Characteristic times of compaction (1) and cooling (2) in obtaining the ceramic hard alloy vs liquid-phase content.

Fig. 14. Characteristic times of compaction (1) and cooling (2) in obtaining powdered-metal hard alloy vs liquid-phase content.

3. The influence of the effective dynamic viscosity of the synthesized hard-alloy material on the process of compaction is studied. It is shown that a decrease in dynamic viscosity is essentially related to the formation of the liquid phase in the synthesis products. In SHS of the hard alloys TiC–TiB_2 and TiB–Ti the increase in the fraction of the liquid phase from 0 to 50 vol.% leads to a decrease in the alloy viscosity from 10^{11} to 10^6 P. The presence of two critical conditions in the composition of a hard alloy due to the generation and existence of the liquid phase is established.

4. A satisfactory qualitative and quantitative agreement of the basic calculated and experimental results is obtained.

NOTATION

a_1, a_2, thermal diffusivity of the hard-alloy material and porosity of the heat insulator; c_1, c_2, mean heat capacity of the liquid phase and of the metal binder; λ_1, λ_2, thermal conductivity of the hard alloy and of the heat insulator; d, D, thickness and diameter of the charge billet; ρ_1, ρ_2, density of the alloy and of the heat insulator; f, external friction coefficient; L, melting heat; $\bar{P}$, mean pressure in the specimen; P_0, pressing pressure at the upper end of the billet; Q, thermal effect of chemical reaction; T_0, initial temperature; T_m, melting temperature; T_c, combustion temperature; t_s, t_c, t_0, time of synthesis, compaction, and cooling of the hard alloy; U, burning rate; ρ, relative density of the hard alloy; η, dynamic viscosity factor of the hard alloy; ξ, lateral pressure coefficient; m, liquid-phase fraction.

LITERATURE CITED

1. A. G. Merzhanov, I. P. Borovinskaya, and F. I. Dubovitskii, Tungsten-Free Hard Alloy and the Method of Its Production, USA Patent No. 4, 431, 448 (1984).
2. A. G. Merzhanov, Self-Propagating High-Temperature Synthesis: Twenty Years of Search and Findings. A Keynote Talk Presented at the International Symposium on Combustion and Plasma Synthesis of High-Temperature Materials, San Francisco (1988).
3. V. A. Shcherbakov, G. A. Vishnyakova, L. V. Kustova, and I. P. Borovinskaya, "Physicomechanical properties of the hard-alloy material STIM-1B/3 produced by the method of SHS pressing," Preprint OIKhF Akad. Nauk SSSR, Chernogolovka (1986).
4. A. G. Merzhanov, in: Physical Chemistry. Current Problems [in Russian], Moscow (1983), pp. 5-45.
5. V. A. Shcherbakov, I. P. Borovinskaya, and A. S. Shteinberg, "The influence of the processes of degassing and heat transfer on compaction of the combustion products in the system Ti–C–B," Preprint OIKhF Akad. Nauk SSSR, Chernogolovka (1986).
6. V. A. Shcherbakov, A. E. Sychev, and A. S. Shteinberg, Fiz. Goreniya Vzryva, No. 4, 55-61 (1986).

7. N. N. Zhilyaeva and L. S. Stel'makh, in: Heat and Mass Transfer in Chemically Reacting Systems [in Russian], Minsk (1989), Part 2, pp. 44-53.
8. V. A. Shcherbakov and A. N. Pityulin, Fiz. Goreniya Vzryva, No. 5, 108-111 (1983).
9. N. P. Novikov, I. P. Borovinskaya, and A. G. Merzhanov, Fiz. Goreniya Vzryva, No. 2, 201-206 (1974).
10. M. S. Koval'chenko, Theoretical Foundations of Hot Treatment of Porous Materials by Pressing [in Russian], Kiev (1980).
11. V. V. Skorokhod, The Rheological Fundamentals of the Theory of Sintering [in Russian], Kiev (1972).
12. Ya. E. Geguzin, Physics of Sintering [in Russian], Moscow (1967).
13. V. V. Skorokhod, Inzh.-Fiz. Zh., **3**, No. 11, 69-71 (1960).
14. R. I. Nigmatulin, Fundamentals of Mechanics of Heterogeneous Media [in Russian], Moscow (1978).
15. A. I. Khvadagiani, V. A. Shcherbakov, G. A. Vishnyakova, et al., "Producing hard alloys on the basis of titanium and zirconium borides by the SHS method with pressing," Preprint OIKhF Akad. Nauk SSSR, Chernogolovka (1985).
16. A. V. Lykov, Theory of Heat Conduction [in Russian], Moscow (1967).
17. H. Carslaw and G. Eger, Thermal Conductivity of Solids [Russian translation], Moscow (1964).
18. V. I. Odelevskii, Zh. Tekh. Fiz., **21**, No. 6, 118-146 (1961).
19. G. I. Dul'nev and B. P. Zarichnyak, Thermal Conductivity of Mixtures and Composite Materials [in Russian], Leningrad (1974).
20. G. V. Samsonov and I. M. Vinitskii, High-Melting Compounds (Handbook) [in Russian], Moscow (1976).
21. B. A. Fridlender, S. S. Ordan'yan, V. S. Neshpor, et al., Teplofiz. Vys. Temp., **18**, No. 5, 1002-1006 (1980).
22. A. I. Emel'yanov and Yu. S. Karimov, Poroshk. Metall., No. 11, 75-79 (1986).